JOURNAL OF MECHANICS OF CONTINUA AND MATHEMATICAL SCIENCES
www.journalimcms.org

ISSN (Online) : 2454 -7190 Vol.-16, No.-4, April (2021) pp 47-60 ISSN (Print) 0973-8975

SIMILARITY SOLUTION OF HEAT AND MASS TRANSFER FOR LIQUID EVAPORATION ALONG A VERTICAL PLATE COVERED WITH A THIN POROUS LAYER

Md. Hasanuzzaman[1], Md. Mosharrof Hossain[2], M.M. Ayub Hossain[3]

[1]Associate Professor, Department of Mathematics, Khulna University of Engineering & Technology, Khulna-9203, Bangladesh

[2]Assistant Professor, Department of Mathematics, Govt. BM College, Barishal-8200, Bangladesh,

[3]Assistant Professor, Department of Mathematics, Shahid Abdur Rab Serniaat Textile Engineering College, Barishal-8200, Bangladesh

[1]hasanuzzaman@math.kuet.ac.bd, [2]mosharrofs77@gmail.com, [3]ayubjpi@gmail.com

Corresponding Author: Md. Hasanuzzaman

https://doi.org/10.26782/jmcms.2021.04.00004

(Received: January 16, 2021; Accepted: March 22, 2021)

Abstract

In this paper, heat and mass transfer for liquid evaporation along a vertical plate covered with a thin porous layer has been investigated. The continuity, momentum, energy and mass balance equations, which are coupled nonlinear partial differential equations are reduced to a set of two nonlinear ordinary differential equations and solved analytically and numerically by using the shooting technique in MATLAB. The effect of various parameters like the Froude number, the porosity, the Darcy number, the Prandtl number, the Lewis number and the driving parameters on the temperature and concentration profiles are presented and discussed. It is viewed that the heat transfer performance is enhanced by the presence of a porous layer. The local Nusselt number and the local Sherwood numbers are computed and analyzed both numerically and graphically.

Keywords: Similarity solution, evaporation, vertical plate, liquid film, porous layer

I. Introduction

Effective latent heat transfer mechanisms are widely utilized in industrial fields such as chemical distillation, air conditioning, cooling towers, drying, and desalination which is liquid film evaporation. With the liquid film exposed to a forced gas stream, the physical scheme consists of a thin liquid film flowing down along a heated plate. Because part of the liquid evaporates into the gas stream, liquid film evaporation possesses a high heat transfer coefficient, low feed rates and other inherent advantages. However, the transport phenomena involve the coupled heat

and mass transfer at the liquid film–gas interface because the theoretical analysis of the liquid film evaporation problem is inherently complicated.

The problem based on simplified 1-D and 2-D mathematical models are usually examined in previous research. [II], [VII], [VIII],[IX] was used the 1-D model to develop the governing conservation of mass, mass species, momentum and energy by the conservation laws to the control volumes of the liquid film and moist air. The heat and mass transfer characteristics in a wet surface heat exchanger are analyzed by MaClaine-Cross and Bank [VIII], [IX]. The experimental data are 20% smaller than their results. A 1-D design methodology for a counter-current falling film evaporative cooler is illustrated by Wassel and Mills [II]. The narrow flow passages were found to be more effective than conventional designs for the thermal performance of the evaporative condenser. Perez-Blanco and Bird [VII] were formulated a 1-D model of heat and mass transfer in the evaporative cooling process that takes place in a single-tube exchanger. In advance, 2-D model composition focused on heat and mass transfer in the gas stream, with the liquid film considered to be at rest and with a very thin constant thickness. For the gas stream, the vaporizing liquid film is treated as the boundary condition [III], [XV] and the temperature distributions across the film are assumed to be linear [XVI], [XVII]. There are many types of research with more rigorous treatments of the equations governing the liquid film and liquid-gas interface that have been published. The evaporative cooling of liquid film through interfacial heat and mass transfer in a vertical channel was studied by Yan and Lin [XIX]. The numerical solution for convective heat and mass transfer along with an inclined heated plate with film evaporation which presented by Yan and Soong [XIX]. The cooling characteristics of a wet surface heat exchanger with a liquid film evaporating into a countercurrent moist airflow which is numerically analyzed by Tsay [XXI]. Neglected inertia in the momentum equation and the normal convection term in the heat equation for liquid film flow, thus the liquid film flow is simplified to a 1-D momentum equation and 1-D (or 2-D) heat equation which is studied the above [XVIII], [XX], [XXI]. Recently Mezaache and Daguenet [V] was studied the complete two-dimensional boundary layer model for the evaporating liquid and gas flows along with an inclined plate. Recently, J.-S. Leu et al. [XI] studied the effect of the porous layer on heat and mass transfer. Their parametric analyses focused on features such as gas inlet conditions and the structural properties of the porous material on the performance of liquid film evaporation. The free convection boundary layer flow of a Darcy–Brinkman fluid induced by a horizontal surface embedded in a fluid-saturated porous layer is explained by Rees and Vafai [V] for the studies of heat and mass transfer for liquid film flow in a porous medium. The fluid flow and heat transfer interfacial conditions between a porous medium and a fluid layer which is detailed analyzed by Alazmi and Vafai [IV]. The coupled heat and mass transfer in a stagnation point flow of air through a heated porous bed with thin liquid film evaporation were studied by Zhao [XVIII]. Also, Zhao [XVIII] assumed the liquid layer was very thin and stationary, and the airstream was idealized as the stagnation point flow pattern to achieve the analytical solution. Khader and Megahed [XII] are presented a numerical technique which is the implicit finite difference method to the search for the numerical solutions for the given equations. Their technique

reduces the problem to a system of algebraic equations. Recently, M. Hasanuzzaman and A. Miyara[XIII] have been studied a possible similarity solution of unsteady natural convection laminar boundary layer flow of viscous incompressible fluid caused by a heated(or cooled) axisymmetric slender body of finite axial length immersed vertically in a viscous incompressible fluid.

The purpose of the present study is, therefore, to find a possible similarity solution of heat and mass transfer for liquid evaporation along a vertical plate covered with a thin porous layer. We are attempted to investigate the effects of several involved parameters on the temperature and concentration fields. The numerical results including the velocity and temperature fields are to be presented graphically for different selected values of the established dimensionless parameters. The local skin friction, local Nusselt number and the local Sherwood numbers are computed numerically and graphically as well as analyzed.

II. Governing Equations

Figure 1 shows the physical model and the coordinates.

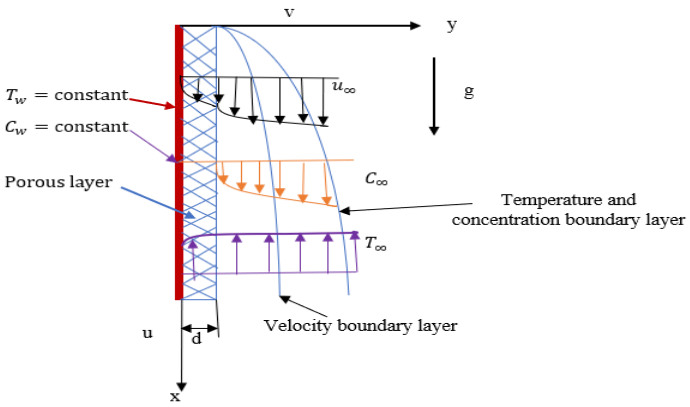

Figure 1: Physical model and coordinates system

Region of liquid film

The order of magnitude analysis showed that the inertia terms in the momentum equation can be neglected as compared with the diffusion term which is under the assumption of the thin liquid film. The transverse direction is much greater than in the longitudinal gradients of velocity and temperature. The continuity, momentum and energy boundary layer equations by including the non-Darcian models of boundary viscous and inertia effects are as follows:

$$\frac{\partial u_l}{\partial x} + \frac{\partial v_l}{\partial y} = 0 \tag{1}$$

$$0 = \rho_l g + \frac{\mu_l}{\varepsilon}\frac{\partial^2 u_l}{\partial y^2} - \frac{\mu_l}{K}u_l - \frac{\rho_l C}{\sqrt{K}}u_l^2 \tag{2}$$

$$u_l \frac{\partial T_l}{\partial x} = \alpha_e \frac{\partial^2 T_l}{\partial y^2} \tag{3}$$

where the subscript "*l*" represents the variables of the liquid stream. ε is the porosity, μ_l is the dynamic viscosity, *K* is the permeability of the porous medium, C is the flow inertia parameter [XIV], ρ_l is density and α_e is the effective thermal diffusivity.

Region of the gas stream

The following two-dimensional laminar continuity, momentum, energy as well as concentration equations can be written as

$$\frac{\partial u_g}{\partial x} + \frac{\partial v_g}{\partial y} = 0 \tag{4}$$

$$u_g \frac{\partial u_g}{\partial x} + v_g \frac{\partial u_g}{\partial y} = \nu_g \frac{\partial^2 u_g}{\partial y^2} \tag{5}$$

$$u_g \frac{\partial T_g}{\partial x} + v_g \frac{\partial T_g}{\partial y} = \alpha_g \frac{\partial^2 T_g}{\partial y^2} \tag{6}$$

$$u_g \frac{\partial \omega}{\partial x} + v_g \frac{\partial \omega}{\partial y} = D \frac{\partial^2 \omega}{\partial y^2} \tag{7}$$

where the subscript "*g*" represents the variables of the gas stream. ω is the mass concentration, ρ is the density, ν is kinematic viscosity, α_g is the thermal diffusivity and *D* is the mass diffusivity of the gas.

Boundary Conditions

The appropriate boundary conditions for the present problem are:

at wall $y = 0$,

$$u_l = 0, v_l = 0\ , T_l = T_w \tag{8}$$

at free stream $y = \infty$,

$$u_g = u_\infty, \quad T_g = T_\infty, \ \ \omega = \omega_\infty \tag{9}$$

at interface $y = d$,

$$u_i = u_{l,i} = u_{g,i}, \ \ T_i = T_{l,i} = T_{g,i} \tag{10}$$

$$v_{g,i} = -\frac{D}{1-\omega_i}\left(\frac{\partial \omega}{\partial y}\right)_i \tag{11}$$

$$\left(\mu_l \frac{\partial u}{\partial y}\right)_{l,i} = \left(\mu_g \frac{\partial u}{\partial y}\right)_{g,i} = \tau_i \tag{12}$$

$$\omega = \omega_i \tag{13}$$

$$q_t'' = -\alpha_e \left(\frac{\partial T_l}{\partial y}\right)_i \text{ and } q_t'' = q_g'' + q_l'' = -\alpha_g \left(\frac{\partial T_g}{\partial y}\right)_i + m_v'' h_{fg} \tag{14}$$

The continuity of shear stress and energy balance at the gas-liquid interface is expressed by eqs. (12) and (14). From the wall the total heat flux q_t'' can be transferred to two modes: one is the sensible heat flux via a gas temperature gradient q_g'' , the other is the latent heat flux via the liquid film vaporization q_l''.

The interfacial evaporating mass flux during the calculated procedure is given by

$$m_v'' = \rho_g v_{g,i} = -\frac{\rho_g D}{1-\omega_i}\left(\frac{\partial \omega}{\partial y}\right)_i \tag{15}$$

And the mass concentration ω_i is expressed as

$$\omega_i = \frac{M_v}{M_g}\frac{p_{v,i}}{p_g} \tag{16}$$

where $p_{v,i}$ is the partial pressure of the saturated vapor at the gas-liquid interface.

S. Ergyn [20] can be evaluated the inlet mass flow rate of the liquid film.

$$m_{l,in} = \frac{\rho_l g}{3\nu_l} d^3 \varepsilon^3 \tag{17}$$

Similarity Transforms

In this paper, we used the relation between stream functions and velocity components for the liquid film and the gas boundary layer which are defined, respectively, by

$$u_l = \frac{\partial \psi_l}{\partial y}, \quad v_l = -\frac{\partial \psi_l}{\partial x} \tag{18}$$

$$u_g = \frac{\partial \psi_g}{\partial y}, \quad v_g = -\frac{\partial \psi_g}{\partial x} \tag{19}$$

are introduced. Eq. (3) is automatically satisfied. We introduce the independent variables η_l and η_g, the dimensionless stream functions $F_l(\eta_l)$ and $F_g(\eta_g)$, the dimensionless temperatures $\theta_l(\eta_l)$ and $\theta_g(\eta_g)$, and the normalized concentration $\phi(\eta_g)$ as

$$\eta_l = y\left(\frac{u_\infty}{\nu_l x}\right)^{\frac{1}{2}}, \qquad \eta_g = (y-d)\left(\frac{u_\infty}{\nu_g x}\right)^{\frac{1}{2}} \tag{20}$$

$$F_l(\eta_l) = \frac{\psi_l}{(\nu_l u_\infty x)^{\frac{1}{2}}}, \qquad F_g(\eta_g) = \frac{\psi_g}{(\nu_g u_\infty x)^{\frac{1}{2}}} \tag{21}$$

$$\theta_l(\eta_l) = \frac{T_i - T_l}{T_i - T_w}, \qquad \theta_g(\eta_g) = \frac{T_{g\infty} - T_g}{T_{g\infty} - T_i}, \qquad \phi(\eta_g) = \frac{\omega - \omega_\infty}{\omega_i - \omega_\infty} \tag{22}$$

Using Eqs. (8)- (22), the mathematical problems defined in equs. (1)-(7) are then transferred into the following set of ordinary differential equations:
Region of the liquid film:

$$0 = \frac{1}{F_r^2} + \frac{1}{\varepsilon}F_l''' - \frac{1}{Da}F_l' - \frac{\Gamma}{Da}F_l'^2 \tag{23}$$

$$\theta_l'' + \frac{1}{2}\mathrm{Pr_l}\eta_l F_l' \theta_l' = 0 \tag{24}$$

Region of the gas stream:

$$F_g''' + \frac{1}{2}F_g F_g'' = 0 \tag{25}$$

$$\theta_g'' + \frac{1}{2} Pr_g F_g \theta_g' = 0 \quad (26)$$

$$\phi'' + \frac{1}{2} Le F_g \phi' = 0 \quad (27)$$

Subject to the boundary conditions:

$$F_l' = 0,\ F_l = 0,\ \theta_l = 1 \quad \text{at}\ \eta_l = 0 \quad (28)$$

$$F_g' = 1, \quad \theta_g = 0,\ \phi = 0 \quad \text{at}\ \eta_g \to \infty \quad (29)$$

The liquid film thickness *d* corresponds to η_{li} which must be a constant for enabling the similarity transformation. Consequently, the compatibility conditions (10)- (14) are transferred as

at $\eta_l = \eta_{li}$, or $\eta_g = 0$:

$$(F_l')_i = \left(F_g'\right)_i \quad (30)$$

$$(\theta_l)_i = 0 \quad (31)$$

$$\left(\theta_g\right)_i = 1 \quad (32)$$

$$\left(F_g\right)_i = \frac{2}{Pr_g Le} \frac{\omega_i - \omega_\infty}{1 - \omega_i} \phi_i' \quad (33)$$

$$\left(F_g''\right)_i = R(F_l'')_i \quad (34)$$

$$\phi = 1 \quad (35)$$

$$(\theta_l')_i = \frac{Pr_l}{Pr_g} \left(\frac{\nu_g}{\nu_l}\right)^{\frac{1}{2}} \left[\frac{T_i - T_{g\infty}}{T_\omega - T_i} \left(\theta_g'\right)_i + \frac{H}{Le} \frac{\omega_i - \omega_\infty}{(1-\omega_i)(T_\omega - T_i)} (\phi')_i\right] \quad (36)$$

where, $Fr = \frac{u_\infty}{\sqrt{gx}}$ is the Froude number, $Da = \frac{Ku_\infty}{\nu_l x}$ is the Darcy number, $\Gamma = \frac{C\sqrt{K}u_\infty}{\nu_l}$ is the dimensionless inertia coefficient of non-Darcy flow, $Pr_l = \frac{\nu_l}{\alpha_e}$ is the Prandtl number in the liquid region, $Pr_g = \frac{\nu_g}{\alpha_g}$ is the Prandtl number in gas stream region and $Le = \frac{\alpha_g}{D}$ is the Lewis number.

Flow Parameters

The physical quantities of interest are the local Nusselt number Nu_x and the local Sherwood number Sh_xwhich are given by:

$$Nu_x = -Re_x^{-\frac{1}{2}} \theta'(0), \quad Sh_x = -Re_x^{-\frac{1}{2}} \phi'(0) \quad (37)$$

where $Re_x = \frac{\nu_l}{x\, u_\infty}$ is the local Reynolds number.

III. Simulation Results and Discussions

By using the shooting technique in MATLAB, the set of ordinary differential equations (23)- (27) with the boundary conditions (28)- (36) are solved numerically. Here the temperature and concentration are determined as a function of coordinate η. To get the solution of differential equations (23)- (27) with the boundary conditions (28)- (36), we have adopted a numerical technique based on

MATLAB. In this simulation, we got some non-dimensional numbers such as the Darcy number *Da*, Froude number *Fr*, Prandtl number *Pr* and Lewis number *Le*. We tried to show the effect of these above parameters on temperature and concentration are plotted in figures (2)- (8). To observe the effect of Darcy number *Da*, the other parameters are constants. Similarly, we observed the effect of the parameters *Fr*, *Pr*, *Le* by taking the rest parameters are constants, respectively.

Figure 2 demonstrates the effect of the Froude number *Fr* on the temperature profiles. It is stated from Fig.2 that with an increase in the Froude number the temperature increases Due to the gravitational effect, with an increase of the gravitational force enhancing the temperature.

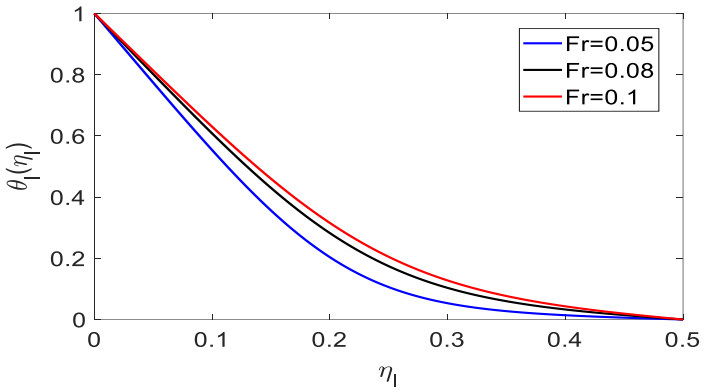

Figure 2: Temperature profiles for different values of Froude number Fr with fixed values $Pr_l = 10, Da = 0.05, \varepsilon = 0.8, \Gamma = 0.5$

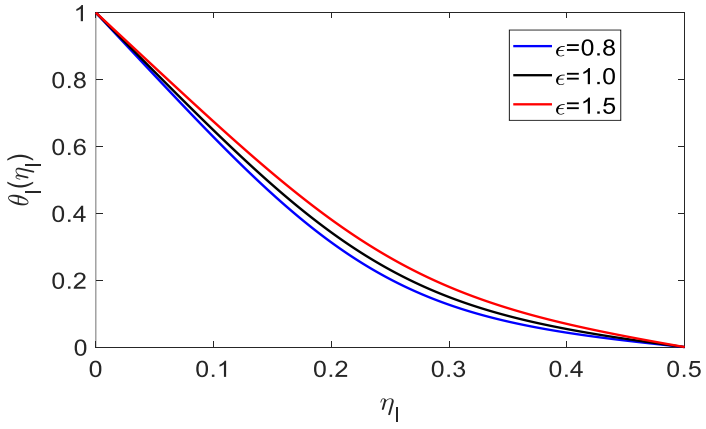

Figure 3: Temperature profiles for different values of porosity ε with fixed values $Pr_l = 10, Da = 0.05, Fr = 0.1, \Gamma = 0.5$

From Fig. 3, illustrate the effect of the porosity ε on the temperature profiles. From Fig. 3, the results show that the temperature increases along the surface within an increase of the porosity. This is due to fact that porosity produces a resistive type of force which causes enhancing the temperature. The effect of the dimensionless inertia coefficient of porous medium Γ on the dimensionless temperature is shown in Fig. 4. From Fig. 4, it is observed that temperature is increased for the increasing value of dimensionless inertia coefficient of porous medium Γ.

The effect of the Darcy number *Da* against η_l on the temperature, the field is shown in Figure 5. From Fig. 5, it is revealed that with an increase in the Darcy number the temperature decreases along η_l. The variation of the dimensionless temperature against η_l for various values of the Prandtl number Pr_l are displayed in Fig.6. Fig. 6 shown that the temperature decreases with the increase of the Prandtl number Pr_l . This is because that fluid with a large Prandtl number possesses high heat capacity, and hence augment the heat transfer.

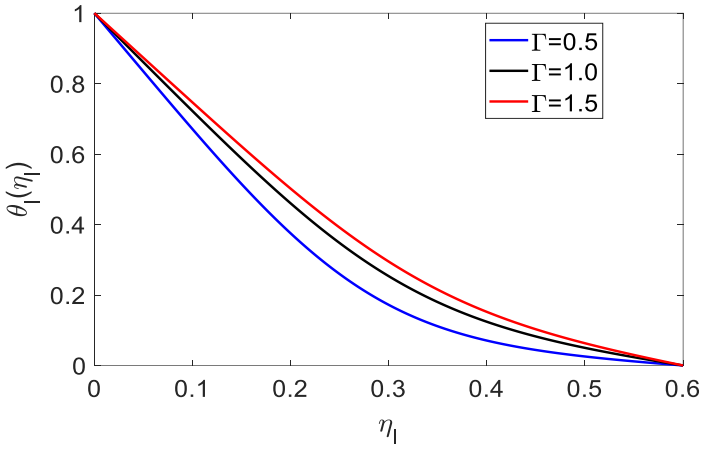

Figure 4: Temperature profiles for different values of dimensionless inertia coefficient of porous medium Γ with fixed values $Pr_l = 10, Da = 0.05, Fr = 0.1, \varepsilon = 0.8$

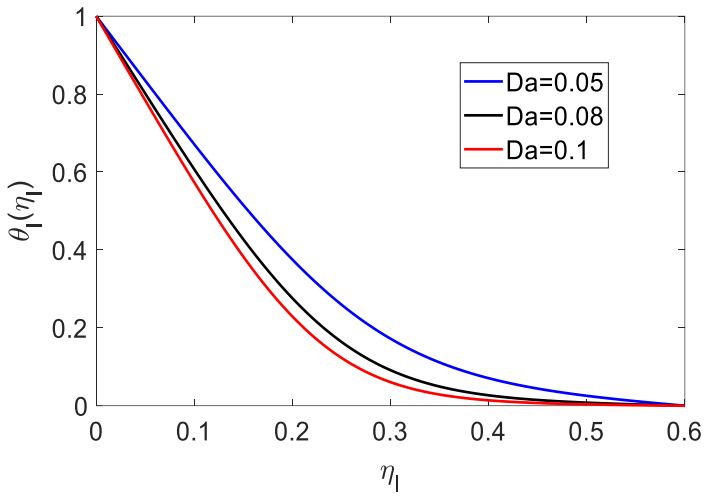

Figure 5: Temperature profiles for different values of Darcy number *Da* with fixed values $Pr_l = 10, Fr = 0.1, \varepsilon = 0.8, \Gamma = 0.5$

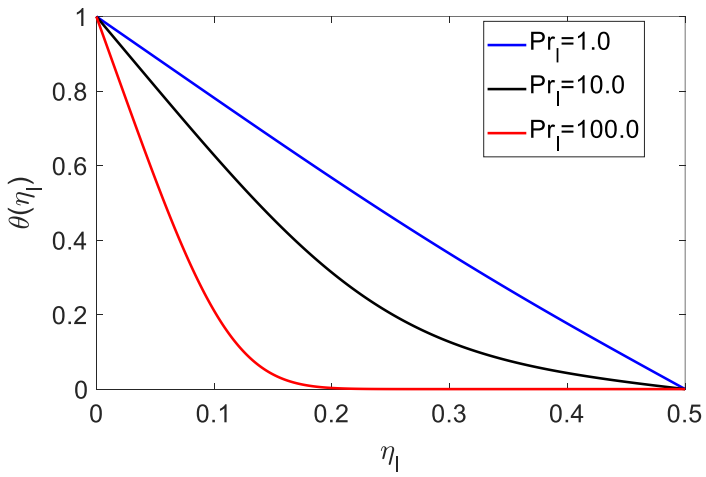

Figure 6: Temperature profiles for different values of Prandtl number Pr_l with fixed values $Da = 0.05, Fr = 0.1, \varepsilon = 0.8, \Gamma = 0.5$

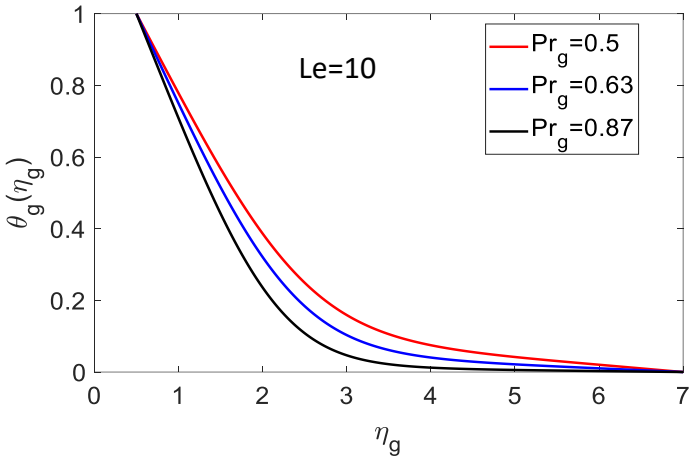

Figure 7: Temperature profiles for different values of Prandtl number Pr_g

For the gas stream region, Fig. 7 demonstrates the effect of the Prandtl number Pr_g on the dimensionless temperature against η_g. It is observed that the temperature decreases with the increase of the Prandtl number Pr_g. This is because in the gas stream region a fluid with a large Prandtl number possesses a large heat capacity and hence augments the heat transfer.

Also, the variation of the dimensionless temperature against η_g for various values of the Lewis number *Le* are displayed in Fig. 8. It is observed that the temperature decreases with the increase of the Lewis number *Le*. This is because with decreases the mass diffusivity the concentration decreases along η_g.

Figure 9 illustrates the effect of Prandtl number Pr_l on the local Nusselt number Nu_x along with the local Reynolds number Re_x. The Prandtl number $Pr_l = \frac{\nu_l}{\alpha_e}$ represents the relative extent of the temperature field. The local Nusselt number increases with an increase in the Prandtl number along with the local Reynold number. This because for increasing the Prandtl numbers larger heat transfer rates are achieved. The Lewis number $Le = \frac{\alpha_g}{D}$, is a dimensionless number defined as the ratio of thermal diffusivity to mass diffusivity. With an increase in the Lewis number the local Sherwood number decrease along with the local Reynolds number. This is because for increasing the Lewis number smaller mass flow rate is achieved which is shown in Fig. 10.

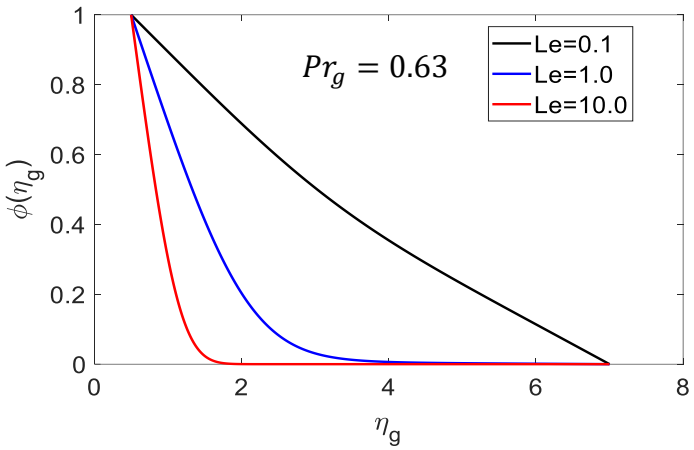

Figure 8: Concentration profiles for different values of Prandtl number *Le*

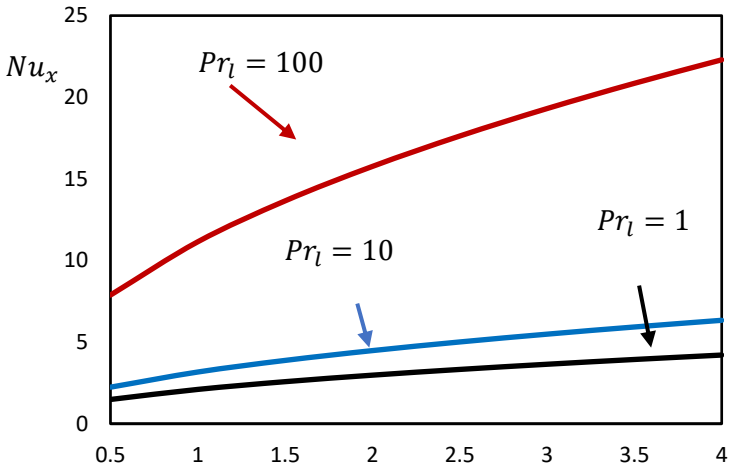

Figure 9: Variation of local Nusselt number Nu_x with Re_x for various Prandtl number Pr_l

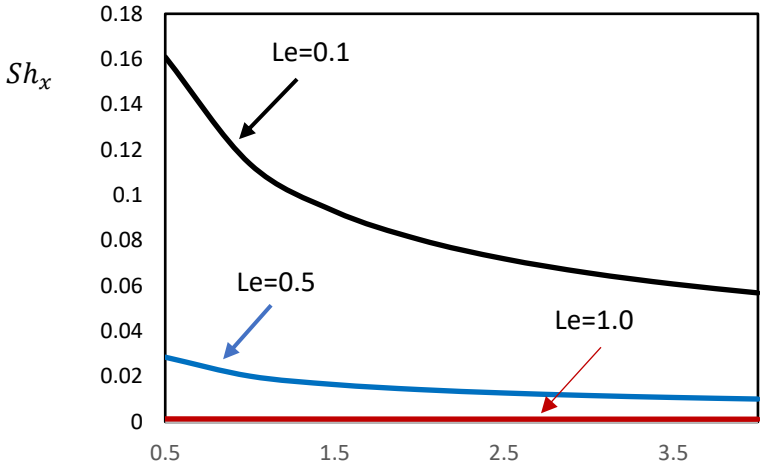

Figure 10: Variation of local Sherwood number Sh_x with Re_x for various Lewis number Le

IV. Conclusions

In this paper, the analytical and numerical solutions of the considered problems have been obtained by using the similarity solution technique in MATLAB. Similarity transformations were used to convert the partial differential equations describing the problem into a system of ordinary differential equations. In the liquid film region, an increase of the gravitational force enhancing the temperature. Also, a fluid with a large Prandtl number possesses high heat capacity, and hence augment the heat transfer. The temperature increases with an increase of the porosity parameter. This is because the porosity produces a resistive type of force which causes an enhancing the temperature. Whereas in the gas stream region, large Prandtl fluids possess lower thermal diffusivity and smaller Prandtl fluids have higher thermal diffusivity. The concentration decreases with an increase in the Lewis number. This is because with decrease diffusivity the concentration decrease. Moreover, the Prandtl number in the liquid region increases the larger heat transfer rate is achieved and the Lewis number increase the smaller mass transfer rate is achieved.

Conflict of Interest:

There is no conflict of interest regarding this article

References

I. A. Ali Hayat, Mohammed R. Salman, : HOMOTOPY PERTURBATION METHOD FOR PERISTALTIC TRANSPORT OF MHD NEWTONIAN FLUID IN AN INCLINED TAPERED ASYMMETRIC CHANNEL WITH THE IMPACT OF POROUS MEDIUM AND CONVECTIVE THERMAL AND CONCENTRATION. *J. Mech. Cont.& Math. Sci*., Vol.-15, No.-9, September (2020) pp 125-141. DOI : 10.26782/jmcms.2020.09.00010

II. A.T. Wassel, A.F. Mills, Design methodology for a counter-current falling film evaporative condenser, ASME J. Heat Transfer 109 (1987) 784–787.

III. B. Gebhart, L. Pera, The nature of vertical natural convection flows resulting from the combined buoyancy effects of thermal and mass diffusion, Int. J. Heat Mass Transfer 14 (1971) 2028–2050.

IV. B. Alazmi, K. Vafai, Analysis of fluid and heat transfer interfacial conditions between a porous medium and a fluid layer, Int. J. Heat Mass Transfer 44 (2001) 1735–1749.

V. D.A.S. Rees, K. Vafai, Darcy–Brinkman free convection from a heated horizontal Surface, Numer. Heat Transfer, Pt A 35 (1999) 191–204.

VI E. Mezaache, M. Daguenet, Effects of inlet conditions on film evaporation along an inclined plate, Solar Energy 78 (2005) 535–542.

VII. H. Peres-Blanco, W.A. Bird, Study of heat and mass transfer in a vertical-tube evaporative cooler, ASME J. Heat Transfer 106 (1984) 210–215.

VIII. I.L. Maclaine-Cross, P.J. Banks, Coupled heat and mass transfer in regenerators-prediction using an analogy with heat transfer, J. Heat Mass Transfer 15 (1972) 1225–1242.

IX. I.L. Maclaine-Cross, P.J. Banks, A general theory of wet surface heat exchangers and its application to regenerative evaporative cooling, ASME J. Heat Transfer 103 (1981) 579–585.

X. J.C. Han, L.R. Glicksman, W.M. Rohsenow, An investigation of heat transfer and friction for rib-roughened surfaces, Int. J. Heat Mass Transfer 21 (1978) 1143–1156.

XI. Jin-Sheng Leu, Jiin-Yuh Jang and Yin Chou, Heat and mass transfer for liquid film evaporation along a vertical plate covered with a thin porous layer, Int. J. Heat and Mass Transfer 49 (2006) 1937–1945.

XII. Khader M. M., Megahed Ahmed M., Numerical simulation using the finite difference method for the flow and heat transfer in a thin liquid film over an unsteady stretching sheet in a saturated porous medium in the presence of thermal radiation, Journal of King Saud University – Engineering Sciences 25(2013), 29 – 34.

XIII. Rafiuddin, Noushima Humera. G., : NUMERICAL SOLUTION OF UNSTEADY TWO - DIMENSIONAL HYDROMAGNETICS FLOW WITH HEAT AND MASS TRANSFER OF CASSON FLUID. *J. Mech. Cont.& Math. Sci*., Vol.-15, No.-9, September (2020) pp 17-30. DOI : 10.26782/jmcms.2020.09.00002

XIV. S. Ergyn, Fluid flow through packed columns, Chem. Eng. Progr. 48 (1952) 89–94.

XV. T.S. Chen, C.F. Yuh, Combined heat and mass transfer in natural convection on inclined surfaces, Numer. Heat Transfer 2 (1979) 233–250.

XVI. T.R. Shembharkar, B.R. Pai, Prediction of film cooling with a liquid coolant, Int. J. Heat Mass Transfer 29 (1986) 899–908.

XVII. T.S. Zhao, Coupled heat and mass transfer of a stagnation point flow in a heated porous bed with liquid film evaporation, Int. J. Heat Mass Transfer 42 (1999) 861–872.

XVIII. W.W. Baumann, F. Thiele, Heat and mass transfer in evaporating two-component liquid film flow, Int. J. Heat Mass Transfer 33 (1990) 267–273.

IX. W.M. Yan, T.F. Lin, Evaporative cooling of liquid film through interfacial heat and mass transfer in a vertical channel—II. Numerical study, Int. J. Heat Mass Transfer 34 (1991) 1113–1124.

XX. W.M. Yan, C.Y. Soong, Convection heat and mass transfer along an inclined heated plate with film evaporation, Int. J. Heat Mass Transfer 38 (1995) 1261–1269.

XXI. Y.L. Tsay, Heat transfer enhancement through liquid film evaporation into countercurrent moist air flow in a vertical plate channel, Heat Mass Transfer 30 (1995) 473–480.